Published in final edited form as:
Chemistry. 2011 May 23; 17(22): 6170–6178. doi:10.1002/chem.201003128.

Stereochemistry and Mechanism of the Brønsted Acid-Catalyzed Intramolecular Hydrofunctionalization of an Unactivated Cyclic Alkene

Rachel E. McKinney Brooner[a] and **Ross A. Widenhoefer**[a]

Ross A. Widenhoefer: rwidenho@chem.duke.edu

[a]Department of Chemistry, Duke University, French Family Science Center, Durham, NC, 27708 (USA), Fax: (+1) (919) 660-1605

Abstract

Through employment of deuterium-labelled substrates, the triflic acid-catalyzed intramolecular *exo*-addition of the X–H(D) (X = N, O) bond of a sulfonamide, alcohol, or carboxylic acid across the C=C bond of a pendant cyclohexene moiety was found to occur, in each case, with exclusive formation (≥90%) of the *anti*-addition product without loss or scrambling of deuterium as determined by ^{1}H and ^{2}H NMR spectroscopy and MS analysis. Kinetic analysis of triflic acid-catalyzed intramolecular hydroamination of *N*-(2-cyclohex-2'-enyl-2,2-diphenylethyl)-*p*-toluenesulfonamide (**1a**) established the second-order rate law: rate = k_2[HOTf][**1a**] and the activation parameters: $\Delta H^{\ddagger}$ = 9.7 ± 0.5 kcal mol^{-1} and $\Delta S^{\ddagger}$ = −35 ± 5 cal K^{-1} mol^{-1}. An inverse α-secondary kinetic isotope effect of k_D/k_H = 1.15 ± 0.03 was observed upon deuteration of the C2' position of **1a**, consistent with partial C–N bond formation in the highest energy transition state of catalytic hydroamination. The results of these studies were consistent with a mechanism for the intramolecular hydroamination of 1a involving concerted, intermolecular proton transfer from an *N*-protonated sulfonamide to the alkenyl C3' position of **1a** coupled with intramolecular *anti*-addition of the pendant sulfonamide nitrogen atom to the alkenyl C2' position.

Introduction

The catalytic addition of the X–H (X = O, N) bond of a nitrogen or oxygen nucleophile across the C=C bond of an electronically unactivated alkene (hydrofunctionalization) represents an attractive and atom economical approach to the formation of C–X bonds.[1] Intramolecular processes are particularly attractive as expedient routes to the synthesis of oxygen and nitrogen heterocycles. Although much of the effort in the area of catalytic alkene hydrofunctionalization has focused on transition metal-based processes, Brønsted acids also catalyze the hydrofunctionalization of C=C bonds, oftentimes with rates and selectivities comparable to transition metal-catalyzed methods.[2–5] For this reason, there is growing concern that a number of metal-based hydrofunctionalization processes, particularly those that employ electrophilic metal complexes or metal triflates in combination with modestly basic nucleophiles, may be catalyzed by Brønsted acid generated under reaction conditions.[5,6]

Distinguishing between transition metal- and Brønsted acid-catalyzed pathways for intramolecular alkene hydrofunctionalization is complicated by a conspicuous gap in our understanding of the mechanisms of Brønsted acid-catalyzed alkene hydrofunctionalization.

Correspondence to: Ross A. Widenhoefer, rwidenho@chem.duke.edu.

Whereas the mechanisms of Brønsted acid-mediated intermolecular alkene hydrofunctionalization have been studied for decades,[7–33] mechanistic information regarding the corresponding intramolecular processes is scarce, and none of the available data pertains to electronically unactivated alkenes. Hosomi has reported that the intramolecular hydroalkoxylation and hydroamination of vinylsilanes with alcohols and sulfonamides occurs with ~85% *syn*-stereoselectivity, which was attributed to intramolecular proton transfer from a protonated nucleophile to the C=C bond of the alkene followed by stereoselective trapping of the more stable β-silylcarbenium rotamer.[34] Hartwig and Schlummer proposed a similar mechanism for the triflic acid-catalyzed intramolecular hydroamination of vinylarenes with sulfonamides involving intramolecular proton transfer from the protonated sulfonamide to the alkene followed by trapping of the resulting benzylic carbenium ion. However, this latter study included neither stereochemical nor kinetic data.[4]

Owing to the considerable current interest in the catalytic intramolecular hydrofunctionalization of electronically unactivated alkenes,[1] we sought to gain information regarding the mechanisms of the Brønsted acid-catalyzed intramolecular hydrofunctionalization of unactivated alkenes. Here we report the stereochemical analysis of the Brønsted acid-catalyzed intramolecular hydrofunctionalization of a cyclohexene moiety with a sulfonamide, alcohol, and carboxylic acid supported by the kinetic analysis of Brønsted acid-catalyzed intramolecular hydroamination. The results of these studies, particularly in the case of intramolecular hydroamination, support a mechanism involving concerted, intermolecular protonation of the alkene coupled with intramolecular *anti*-addition of the pendant nucleophile.

Results

Stereochemistry of Hydroamination

To evaluate the stereoselectivity of Brønsted acid-catalyzed intramolecular alkene hydroamination, we targeted the doubly deuterium-labelled γ-alkenyl sulfonamide *N*-(2-1', 3'-dideuteriocyclohex-2'-enyl-2,2-diphenylethyl)-*p*-toluenesulfonamide (**1a**-1’,3’-d_2) that has been previously employed to evaluate the stereoselectivity of gold(I)-catalyzed alkene hydroamination.[35] Treatment of **1a**-1’3’-d_2 (83 ± 1% d_2, 17% d_1 by MS, ~85% deuterated at C3' by ^{1}H NMR) with a catalytic amount of triflic acid (5 mol %) in toluene at 85 °C for 48 h led to 5-*exo* hydroamination with isolation of **2a**-3a,7$_{eq}$-d_2 (83 ± 1% d_2, 16% d_1 by MS) as the exclusive dideuterated isotopomer in 96% yield without loss of deuterium (eq 1).[36] Single crystal X-ray analysis of protio isotopomer **2a** revealed a *cis*-fused chair cyclohexane with an equatorial diphenylalkyl substituent and an axial sulfonamide substituent.[37] High-field ^{1}H NMR (Figure 1, spectrum a), ^{1}H-^{1}H COSY, and ^{1}H-^{1}H NOESY analysis confirmed that the solid-state conformation of **2a** was preserved in solution and allowed unambiguous assignment of all aliphatic proton resonances.[38] Integration of the H7$_{eq}$ resonance at δ = 2.49 in the ^{1}H NMR spectrum of **2a**-3a,7$_{eq}$-d_2 revealed ~85% deuteration at this position (Figure 1, spectrum b). More importantly, ^{2}H NMR analysis of **2a**-3a,7$_{eq}$-d_2 displayed a ~1:1 ratio of resonances at δ = 2.95 (C3a) and δ = 2.49 (C7$_{eq}$) with no detectable deuteration at either the C7$_{ax}$ (δ ≈ 1.58) or C7a (δ 3.73) positions (Figure 1, spectrum c). Together, these observations established the net *anti*-addition of the N–H bond across the pendant C=C bond of **1a**-1’,3’-d_2 without loss or scrambling of deuterium.

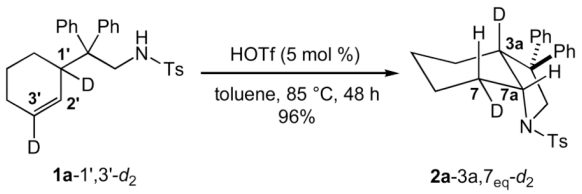

1a-1',3'-d_2 **2a**-3a,7_{eq}-d_2

eq 1

To corroborate the findings outlined in the preceding paragraph, we evaluated the stereoselectivity of the acid-catalyzed intramolecular deuterioamination of *N*-deuterated isotopomer **1a**-*N*-*d*.[39] Treatment of **1a**-*N*-*d* (~90% *d* by ^{1}H NMR) with a catalytic amount of DOTf (5 mol %) at 85 °C in toluene for 48 h led to isolation of **2a**-7_{ax}-d_1 (90 ± 1% *d* by MS) as the exclusive deuterated isotopomer in 77% yield (eq 2). Integration of the H7_{eq} resonance at δ = 2.49 in the ^{1}H NMR spectrum of **2a**-7_{ax}-d_1 revealed no significant deuteration at this position (Figure 1, spectrum d), while ^{2}H NMR analysis displayed a single resonance at δ = 1.58 corresponding to deuteration of the $C7_{ax}$ position with no detectable deuteration at either the $C7_{eq}$ (δ = 2.49) or C7a (δ = 3.73) positions (Figure 1, spectrum e).

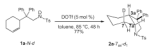

eq 2

The absence of deuterium incorporation into the C7a and $C7_{eq}$ positions of **2a**-7_{ax}-d_1 in the DOTf-catalyzed cyclization of **1a**-*N*-*d* argues against reversible deuteronation of the C2' or C3' carbon atoms of the cyclohexenyl moiety prior to cyclization. To further probe for reversible protonation/deuteronation of the alkene prior to cyclization, the reaction of **1a**-*N*-*d* (~90% *d*) and a catalytic amount of DOTf (5 mol %) at 60 °C in toluene was monitored periodically by ^{2}H NMR spectroscopy and quenched at ~50% conversion by addition of triethylamine. A similar experiment utilizing ^{1}H NMR analysis of a mixture of **1a**-*N*-*d* (~90% *d*) and DOTf (5 mol %) in toluene-d_8 was run concurrently. ^{1}H and ^{2}H NMR analysis of the respective solutions revealed no positional isomerization and no detectable incorporation of deuterium into the C2' or C3' positions (δ = 5.68 and 5.58) of **1a**-*N*-*d*. These observations, together with those outlined above, argue strongly against reversible deuteronation of either the cyclohexene C2' or C3' carbon atom prior to cyclization.

Stereoselectivity of Hydroalkoxylation and Hydroacyloxylation

We extended our stereochemical analysis of acid-catalyzed alkene hydrofunctionalization to include catalytic hydroalkoxylation and hydroacyloxylation employing an approach similar to that employed for intramolecular hydroamination. In one experiment, treatment of the γ-alkenyl alcohol **1b**-1',3'-d_2 (96% d_2 by MS) with a catalytic amount of triflic acid (5 mol %) led to 5-*exo* hydroalkoxylation to form **2b**-3a,7_{eq}-d_2 in 96% isolated yield as the exclusive dideuterated isotopomer with no loss or scrambling of deuterium (95% d_2 by MS) (eq 3). ^{1}H and ^{2}H NMR analysis of **2b**-3a,7_{eq}-d_2 revealed ≥95% deuteration of the $C7_{eq}$ (δ = 1.89) and C3a (δ = 2.71) positions with no detectable deuteration at the $C7_{ax}$ (δ = 1.34) or C7a (δ = 4.12) positions (Figure 2). Similarly, treatment of β-alkenyl carboxylic acid **1c**-1',3'-d_2 (>99% d_2 by MS) with a catalytic amount of triflic acid (5 mol %) led to 5-*exo* hydroacyloxylation to form **2c**-3a,7_{eq}-d_2 as the exclusive dideuterated isotopomer (>98% d_2 by MS) in quantitative yield (eq 4). ^{1}H and ^{2}H NMR analysis of **2c**-3a,7_{eq}-d_2 revealed ≥95% deuteration of the $C7_{eq}$ (δ = 2.16) and C3a (δ = 3.07) positions with no detectable

deuteration at the $C7_{ax}$ (δ = 1.55) or C7a (δ = 4.61) positions (Figure 3). In both cases, these results established the net *anti*-addition of the O–H bond across the C=C bond of the cyclohexene moiety.

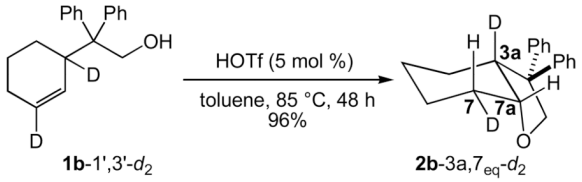

1b-1',3'-d_2 **2b**-3a,7_{eq}-d_2

eq 3

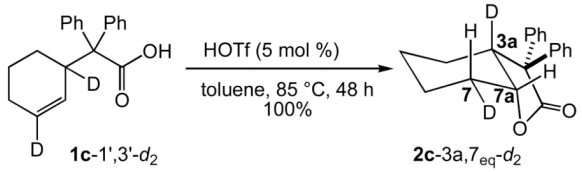

1c-1',3'-d_2 **2c**-3a,7_{eq}-d_2

eq 4

Effect of Solvent and Acid on Hydrofunctionalization

The efficiency and stereoselectivity of Brønsted acid-catalyzed intramolecular hydrofunctionalization was evaluated as a function of acid and solvent at 85 °C (Table 1).Treatment of substrates **1**-1',3'-d_2 with a catalytic amount of triflic acid (5 mol %) in diglyme at 85 °C for 48 h led, in each case, to complete consumption of starting material to form 5-*exo* hydrofunctionalization products **2**-3a,7_{eq}-d_2 as the exclusive dideuterated isotopomers (Table 1, entries 1 – 3). In comparison, reaction of substrates **1**-1',3'-d_2 with triflic acid in acetonitrile effected a significant decrease in reaction rate but led, in each case, to formation of 5-*exo* hydrofunctionalization products **2**-3a,7_{eq}-d_2 as the exclusive isotopomers (Table 1, entries 4 – 6). Attempts to cyclize substrates **1**-1',3'-d_2 with weaker acids such HCl or trifluoroacetic acid (TFA) in toluene at 85 °C for 48 h gave low conversions (Table 1, entries 7 – 12).

Kinetics of Hydroamination

We sought to gain additional information regarding the mechanism of Brønsted acid-catalyzed hydroamination through kinetic analysis of the triflic acid-catalyzed conversion of **1a** to **2a**. To this end, reaction of **1a** (0.50 M) with a catalytic amount of HOTf (25 mM) in toluene at 62 °C was analyzed periodically by liquid chromatography. A plot of ln[**1a**] versus time was linear to ~3 half lives with an observed rate constant of $k_{obs} = 4.2 \pm 0.1 \times 10^{-3}$ s^{-1}, which established the first-order dependence of the rate on [**1a**] (Figure 4; Table 2, entry 1). To determine the dependence of the rate on triflic acid concentration, observed rate constants for the conversion of **1a** to **2a** were determined at [HOTf] = 5.0 and 12.6 mM (Figure 4; Table 2, entries 2 and 3). A plot of k_{obs} versus [HOTf] was linear (Figure 5), which established the first-order dependence of the rate on [HOTf] and the second-order rate law: rate = k_2[**1a**][HOTf] where $k_2 = 1.37 \pm 0.04 \times 10^{-1}$ M^{-1} s^{-1} ($\Delta G^{\ddagger}_{336K} = 21.2 \pm 0.1$ kcal mol^{-1}). To determine the activation parameters for the triflic acid-catalyzed conversion of **1a** to **2a**, second-order rate constants for the conversion of **1a** to **2a** were determined as a function of temperature from 39 to 72 °C (Table 2, entries 4–7). An Eyring plot of these data provided the activation parameters: $\Delta H^{\ddagger} = 9.7 \pm 0.5$ kcal mol^{-1} and $\Delta S^{\ddagger} = -34 \pm 5$ cal K^{-1} mol^{-1} (Figure 6).

Hartwig and Schlummer have shown that *N*-alkyl-*p*-toluenesulfonamides are quantitatively protonated by triflic acid,[4] consistent with the significantly greater acidity of HOTf ($pK_a \approx -15$) relative to a protonated sulfonamide ($pK_a \approx -5$);[40–42] it is also known that sulfonamides are protonated at nitrogen rather than at oxygen.[43] Therefore, the active catalytic species in the conversion of **1a** to **2a** is most likely an *N*-protonated sulfonamide. Laughlin[41] and Olavi *et al*.[42] have shown that the conjugate acids of *N*-alkyl sulfonamides are more acidic than are the conjugate acids of *N*,*N*-dialkyl sulfonamides by ~0.5 pK_a (H_0) units. However, if **1a**•HOTf were more acidic than **2a**•HOTf, deviation from first-order behavior in the conversion of **1a** to **2a** would be observed due to the changing composition of the acidic species with increasing conversion. Because no significant deviation from linearity was observed in any of the pseudo first-order plots for the conversion of **1a** to **2a** (Figure 4), it appears that acidity and/or reactivity of **1a**•HOTf and **2a**•HOTf are not significantly different. For these reasons, the rate law for the conversion of **1a** to **2a** of k_2[**1a**][HOTf] is more appropriately described as rate = k_2[**1a**][R_2NTs•HOTf] [R_2NTs = **1a** and **2a**].

α-Secondary Kinetic Isotope Effect

α-Secondary kinetic isotope effects (KIEs) have been utilized to probe for transition state rehybridization in the elucidation of a range of organic reaction mechanisms.[44] As was outlined by Steitwieser,[45] α-secondary KIEs are typically attributed to changes in the stretching and bending frequencies of a C–H bond undergoing ground state → transition state rehybridization.[46] Because C–H stretching and in-plane bending frequencies differ little between sp^3 and sp^2 centers, α-KIEs arise primarily from the significantly higher out-of-plane bending frequency of an sp^3 C–H bond (~1340 cm^{-1}) relative to an sp^2 C–H bond (~800 cm^{-1}), which produces a normal KIE in the case of $sp^3 \rightarrow sp^2$ rehybridization and an inverse KIE in the case of $sp^2 \rightarrow sp^3$ rehybridization.

To probe for rehybridization of the C2' carbon atom of the cyclohexenyl moiety in the transition state of the turnover-limiting step of the triflic acid-catalyzed hydroamination of **1a**, we determined the α-secondary KIE resulting from deuteration of the C2' carbon of the cyclohexenyl moiety employing deuterated isotopomer **1a**-2'-d_1. Owing to the small magnitude of secondary KIEs[44] and to avoid errors associated with variations in catalyst concentration and temperature, the α-secondary KIE was determined though a competition experiment. To this end, a ~1:1 mixture of **1a** and **1a**-2'-d_1 and a catalytic amount of HOTf (5 mol %) in toluene was heated at 60 °C and analyzed periodically by LCMS. The concentrations of **1a** and **1a**-2'-d_1 were determined from total conversion and from the isotopic ratios **1a:1a**-2'-d_1 and **2a:2a**-7a-d_1. Plots of ln[**1a**] and ln[**1a**-2'-d_1] versus time were linear to ~3 half lives with observed rate constants of $k_{obs} = 2.19 \pm 0.03 \times 10^{-3}$ s^{-1} and $2.51 \pm 0.05 \times 10^{-3}$ s^{-1}, respectively (Figure 7), which correspond to an inverse KIE of $k_D/k_H = 1.15 \pm 0.03$. In a separate experiment, treatment of **1a**-2'-d_1 (75 ± 1 % d_1 by MS) with a catalytic amount of HOTf (5 mol %) at 85 °C in toluene for 48 h led to isolation of **2a**-7a-d_1 (76 ± 1% *d* by MS) as the exclusive deuterated isotopomer in 77% yield without detectable loss or scrambling of deuterium as determined by MS and ^{2}H NMR analysis (eq 5; Figure 1, spectrum f).

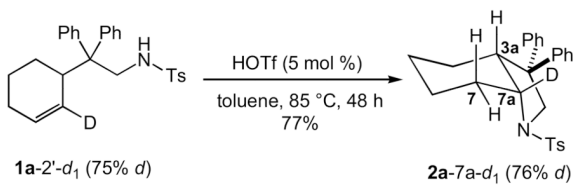

1a-2'-d_1 (75% *d*) **2a**-7a-d_1 (76% *d*)

eq 5

Discussion

Mechanisms of Intermolecular Electrophilic Alkene Hydrofunctionalization

Extensive kinetic analyses of the Brønsted acid-catalyzed hydration and intermolecular hydroalkoxylation of conjugated and non-conjugated alkenes reveals that with few exceptions, these transformations occur via irreversible, turnover-limiting protonation of the C=C bond followed by nucleophilic trapping of a solvated carbenium ion intermediate.[7] Although early work by Taft suggested that proton transfer was preceded by reversible formation of a π-protonium complex,[8] this hypothesis has been largely discounted.[7,9] Deviations from the general hydration mechanism are rare but may occur in the cases of particularly long-lived or short-lived carbenium ions. For example, mechanisms involving rapid and reversible C=C protonation followed by rate-limiting nucleophilic addition to the resulting carbenium ion have been documented in the cases of highly stabilized carbenium ions.[10]

Drawing from the analyses of Jencks,[11] Kresge posited that preassociation or concerted mechanisms for alkene hydration may be enforced by short carbenium ion lifetimes.[12] On the basis of this analysis, Kresge considered, but ultimately discounted, a preassociation pathway for the acid-catalyzed hydration of *trans*-cyclooctene; however, Kresge also suggested that preassociation pathways may be operative for the hydration of unstrained olefins that generate secondary carbenium ions in dilute acid conditions.[12] Similarly, consideration of carbenium ion lifetimes led both Jencks[13] and Herlihy[14] to propose concerted pathways for the hydration of monosubstituted alkenes under dilute acid conditions, although in neither case were these pathways rigorously established.

The mechanisms of the addition of hydrogen halides to alkenes and the addition of acetic acid to non-conjugated alkenes catalyzed by hydrogen halides and related Brønsted acids have also been investigated.[15–32] These transformations typically occur with ~85% *anti*-selectivity in the case of non-conjugated acyclic alkenes and with >95% *anti*-selectivity in the case of non-conjugated cyclic alkenes.[16–25,27] Hydrogen halide addition typically obeys the ternary rate law: rate = k[alkene][HX]^2, whereas the acid-catalyzed hydroacetoxylation typically obeys the binary rate law: rate = k[alkene][HX].[17–19,26–29] Both Ad_E3 pathways involving concerted C–H and C–X (X = halide or OAc) addition across the C=C bond of the alkene[16,18,19,22,23,25,27,28] and/or stepwise Ad_E2 pathways involving rate-limiting, halide assisted protonation of the alkene followed by rapid trapping of a tight carbenium ion pair have been proposed to account for these observations.[17,18,22,25,26,29] Initial formation of a π-protonium complex has also been invoked[16,24,25] but, as was the case for alkene hydration, little direct evidence supports these hypotheses.[30]

In contrast to the behavior of weaker Brønsted acids, Roberts reported that the HOTf-catalyzed addition of acetic acid-*O*-*d* to cyclopentene was non-stereoselective.[31] In a separate study, Pasto reported that the HOTf-catalyzed addition of acetic acid-*O*-*d* to 2-butene occurred with modest (57–72%) *anti*-stereoselectivity and was accompanied by alkene isomerization and H/D exchange.[23] The latter transformation was proposed to occur through an Ad_E2 pathway involving reversible formation of a carbenium ion pair that was trapped by acetic acid. The slight preference for *anti*-addition was attributed to steric shielding of the *syn* face of the carbenium ion in the tight ion pair. In comparison, the addition of hydrogen halides to cyclic and acyclic vinyl arenes occurs with up to 90% *syn*-selectivity in low-polarity solvents such as dichloromethane.[32] This behavior is in accord with a stepwise Ad_E2 pathway involving turnover-limiting protonation to form a tight ion pair that undergoes rapid collapse (*syn*-addition) or rearrangement followed by collapse (nonselective).

Recently, the mechanisms of triflic acid-catalyzed intermolecular alkene hydrofunctionalization with phenols and protected amines has been investigated by a pair of DFT studies.[33] In both cases, calculations predict a concerted, *syn*-addition of H–X (X = N, O) bond of the nucleophile across the C=C bond of the alkene via an eight-membered cyclic transition state in which triflic acid interacts with both the alkene and the nucleophile.[33]

Mechanism of Acid-Catalyzed Conversion of 1a to 2a

Our experimental observations rule out several potential mechanisms for the acid-catalyzed conversion of **1a** to **2a**. The absence of deuterium scrambling, alkene isomerization, and/or incorporation of deuterium into unreacted starting material in the acid-catalyzed reactions of isotopomers **1a**-1',3'-d_2, **1a**-*N*-*d*, and **1a**-2'-d_1 argues strongly against mechanisms involving rapid and reversible protonation/deuteronation of the C2' or C3' alkenyl carbon atoms followed by turnover-limiting attack of the pendant sulfonamide on a C2' carbenium ion. Furthermore, the *anti*-stereoselectivity and second-order rate law for the conversion of **1a** to **2a** rule out a mechanism analogous to those proposed by Hosomi[35] and Hartwig[4] involving intramolecular proton transfer from a protonated sulfonamide to the C3' alkenyl carbon atom followed by trapping of the resulting carbenium ion with the neutral sulfonamide moiety.

We therefore considered mechanisms for the acid-catalyzed conversion of **1a** to **2a** initiated by turnover-limiting, irreversible intermolecular proton transfer from a protonated sulfonamide to the C3' alkenyl carbon of **1a**. Of the possible mechanisims that meet this requirement, stepwise pathways involving a solvationally equilibrated carbenium ion (Ad_E2) or a tight ion pair are inconsistent with our experimental observations, as is a stepwise preassociation pathway. Because the regio- and stereoselectivity of C–N bond formation in the conversion of **1a** to **2a** is largely predetermined by substrate geometry, protonation must occur regio- and stereoselectively at the C3' position of the cyclohexene moiety on the face opposite that occupied by the diphenylethylsulfonamide group. Although delivery of a proton to the less sterically hindered face of the alkene is reasonable, regioselective protonation of the electronically unbiased C=C bond at C3' without participation of the pendant sulfonamide group appears unlikely. Preassociation of the sulfonamide nitrogen atom and alkene C2' atom prior to intermolecular proton transfer to C3' in a manner analogous to that suggested by Kresge[12] accounts for the regioselectivity of proton transfer only if the nitrogen atom is felt in the transition state for protonation, at which point, C–H and C–N bond formation become concerted.[11]

Key to distinguishing between stepwise and concerted mechanisms for the conversion of **1a** to **2a** is the α-secondary KIE of $k_D/k_H = 1.15 \pm 0.03$ determined for the conversion of **1a**-2'-d_1 to **2a**-7a-d_1. This observation points to significant C–N bond formation in the turnover-limiting step of hydroamination and argues strongly against a stepwise pathway involving turnover-limiting carbenium ion formation. Employing Streitwieser's approximation[45] of the Bigeleisen equation[47] and representative C–H stretching and bending frequencies for the sp^2 carbon of *cis*-2-butene as a model for **1a** and the sp^3 methine carbon of a secondary alcohol as a model for **2a**,[48,49] we estimate a maximum α-secondary KIE for the conversion of **1a** to **2a** resulting from conversion of an alkene ground state to a tetrahedral transition state of $k_D/k_H \approx 1.20$ at 333 K. Consideration of calculated fractionation factors for H/D exchange between olefinic and aliphatic positions predicts a similar value.[50] Conversely, because conversion of **1a** to **2a** via turnover-limiting carbenium ion formation would occur without transition state rehybridization, such a process should occur without a significant α-secondary KIE. Supporting this contention, the calculated fractionation factor of 1.179 for H/D exchange between a secondary carbenium ion and secondary alkyl moiety indicates that fractionation factors between an olefinic and carbenium hydrogen differ by only a few percent.[51]

Available experimental data regarding the α-secondary KIEs of the Brønsted acid-promoted addition of nucleophiles to alkenes are in accord with the analysis provide above. For example, the thiocyanate-catalyzed isomerization of maleic acid-d_2 to fumaric acid-d_2 displayed an inverse KIE of $k_D/k_H = 1.17$ (corrected for H/D exchange) at 25 °C, attributed to turnover-limiting conjugate addition of thiocyanate to an *O*-protonated maleic acid.[52] In contrast, acid-catalyzed hydration of α-deuteriostyrene[53] or 4,4-dideuterio-1-phenyl-1,3-butadiene[54] displayed no detectable KIE, consistent with turnover-limiting carbenium ion formation. Acid-catalyzed hydrolysis of ethyl vinyl ether produced a small inverse α-secondary KIE of $k_D/k_H = 1.036 \pm 0.004$; however, this effect was attributed to an inductive KIE rather than to an α-secondary KIE.[55]

All of our experimental observations, including the second-order rate law, activation parameters, inverse α-secondary KIE, and *anti*-stereoselectivity are consistent with a concerted mechanism for the conversion of **1a** to **2a**. Our proposed mechanism is depicted in Scheme 1 for the DOTf-catalyzed conversion of **1a**-*N*-*d* to **2a**-7_{ax}-d_1. As has been noted by Jencks,[11] preassociation is a necessary prerequisite for concerted reaction pathways and, as such, conversion of **1a**-*N*-*d* to **2a**-7_{ax}-d_1 is likely initiated by formation of the alkene-sulfonamide encounter complex **I**. Intermolecular deuteron transfer from an *N*-deuterated sulfonamide to the C3' alkenyl carbon atom of **1a**-*N*-*d* in concert with intramolecular *anti*-addition of the pendant sulfonamide nitrogen atom to the C2' alkenyl carbon atom via transition state **TS-I** would generate the *N*-deuterated sulfonamide cation **2a**-7_{ax}-d_1•DOTf. Intermolecular deuteron transfer from **2a**-7_{ax}-d_1•DOTf either to a second sulfonamide nitrogen atom or to the C3' carbon atom of a second molecule of **1a**-*N*-*d* would release **2a**-7_{ax}-d_1 and continue the catalytic cycle (Scheme 1).

Conclusion

We have shown that the Brønsted acid-catalyzed intramolecular hydrofunctionalization of a cyclohexenyl moiety with a sulfonamide, alcohol, or carboxylic acid occurs with net *anti*-addition of the H–X (X = N, O) bond across the pendant C=C bond of the cyclohexene moiety and without positional isomerization or H/D exchange. Kinetic analysis of the intramolecular hydroamination of cyclohexenyl sulfonamide derivative **1a** established a second-order rate law and large negative entropy of activation. Kinetic analysis of the intramolecular hydroamination of deuterated isotopomer **1a**-3'-*d* revealed an inverse α-secondary KIE of $k_D/k_H = 1.15 \pm 0.03$, consistent with significant C–N bond formation in the turnover-limiting step of hydroamination. All of our experimental observations regarding the Brønsted acid-catalyzed the conversion of **1a** to **2a** support a mechanism involving concerted intermolecular transfer of a proton from an *N*-protonated sulfonamide to the C3' carbon atom of **1a** coupled with intramolecular *anti*-addition of the pendant sulfonamide nitrogen atom to the C2' carbon atom. The high *anti*-stereoselectivity and absence of deuterium scrambling in the Brønsted acid-catalyzed intramolecular hydroalkoxylation of **2b**-1',3'-d_2 and hydroacyloxylation of **2c**-1',3'-d_2 suggests that these transformations occur via a similar pathway.

Perhaps the most significant implication of our study is that the stereoselectivity of these Brønsted acid-catalyzed intramolecular hydrofunctionalization processes is indistinguishable from that expected for an outer-sphere transition metal-catalyzed pathway.[56] Furthermore, in the event that Brønsted acid were generated stoichiometrically from a metal precursor, the resulting acid-catalyzed intramolecular hydrofunctionalization would appear to conform to the second-order rate law: rate = [metal][substrate], apparently consistent with a metal-catalyzed cyclization. The absence of positional isomerization or olefinic H/D exchange would also appear consistent with a metal-catalyze transformation. As a result, it appears that strong corroborating evidence and/or rigorous control experiments are required to

confidently discount the presence of Brønsted acid-catalyzed reaction pathways in metal-based alkene hydrofunctionalization processes.

Unknown at this time is the effect of substrate structure on the mechanism of Brønsted acid-catalyzed intramolecular alkene hydrofunctionalization, such as in the cases of acyclic alkenes or conjugated alkenes. Further studies in this area will probe the stereochemistry and mechanisms of these permutations of acid-catalyzed alkene hydrofunctionalization.

Experimental Section

General procedure for acid-catalyzed hydrofunctionalization

Synthesis of 2a.[35] Triflic acid (0.7 μL, 7.5×10^{-3} mmol) was added via syringe to a solution of **1a** (64.7 mg, 0.150 mmol) in toluene (0.3 mL). The resulting solution was heated at 60 °C for 3 h, cooled to room temperature, and filtered through a plug of silica gel. Solvent was evaporated under vacuum to give pure **2a** (64.5 mg, 100 %) as a white solid. The aliphatic protons of **2a** were unambiguous assigned on the basis of combined ^{1}H–^{1}H 800 MHz COSY and ^{1}H–^{1}H NOESY analysis at 45 °C in $CDCl_3$ (See Supporting Information).[38] ^{1}H NMR (800 MHz, $CDCl_3$, 45 °C): δ 7.43 (d, *J* = 8.0 Hz, 2 H), 7.19 (t, *J* = 8.0 Hz, 2 H), 7.09 (t, *J* = 8.0 Hz, 1 H), 7.07 - 6.98 (m, 9 H), 4.48 (d, *J* = 11.1 Hz, 1 H; *H2*), 4.25 (d, *J* = 11.1 Hz, 1 H; *H2*), 3.78 (m, 1 H; *H7a*), 2.95 (dt, *J* = 10.4, 4.8 Hz, 1 H; *H3a*), 2.49 (br d, *J* = 14.4 Hz, 1 H; $H7_{eq}$), 2.32 (s, 3 H), 1.58 (m, 1 H; $H7_{ax}$), 1.55–1.41 (m, 4 H; *H5* and *H6*), 1.28–1.15 (m, 2 H; *H4*). ^{13}C{^{1}H} NMR (126 MHz, $CDCl_3$, 25 °C): δ 145.1, 143.8, 142.8, 134.2, 129.3, 128.5, 128.4, 127.6, 127.1, 126.7, 126.1, 125.7, 59.1, 58.2, 55.5, 44.3, 28.8, 25.5, 24.5, 21.5, 20.1.

All remaining acid-catalyzed hydrofunctionalization reactions were performed employing analogous procedures.

Kinetic Experiments

Triflic acid (5.00 μL, 5.6×10^{-2} mmol, 25 mM) was added via a gas-tight syringe equipped with a stainless steel needle into a solution of **1a** (488 mg, 1.13 mmol, 0.50 M) in dry toluene (2.25 mL) that had been pre-equilibrated at 62.5 °C. The reaction mixture was stirred and aliquots were periodically removed via syringe, quenched with saturated aqueous $NaHCO_3$, extracted with acetonitrile, and analyzed by liquid chromatography equipped with a UV detector. The conversion of **1a** to **2a** was quantitative and occurred without formation of intermediates or byproducts. Furthermore, analysis of stock solutions of **1a** and **2a** revealed that the UV response factors of **1a** and **2a** were not significantly different (≤ 0.1%) over the concentration range utilized in these experiments. For these reasons, the concentration of **1a** was determined from the integration of the peaks in the LC spectrum corresponding to **1a** and **2a** according to the formula [**1a**] = 0.50 M × {[**1a**]/[**1a**] + [**2a**]}. A plot of ln[**1a**]*t* versus time was linear to ~3 half-lives (Figure 4, Table 2), with an observed rate constant of $k_{obs} = 4.2 \pm 0.1 \times 10^{-3}$ s^{-1}. Employing a similar procedure, observed rate constants for the reaction of **1a** with triflic acid were determined as a function of [HOTf] and temperature

α-Secondary KIE for the conversion of 1a to 2a

A mixture of **1a** (162 mg, 0.376 mmol) and **1a**-2'-d_1 (74% d_1, 326 mg, 0.754 mmol) was dissolved in toluene (2.25 mL). Mass spectral analysis of the resulting solution revealed a 47.6:52.4 mixture of d_0:d_1 isotopomers. The solution was equilibrated at 59.5 °C and triflic acid (4.0 mg, 5.7×10^{-2} mmol) was added. The resulting solution was stirred and aliquots were removed periodically via syringe, quenched with saturated aqueous $NaHCO_3$, extracted with acetonitrile, and analyzed by LCMS for conversion and isotopic abundance.

The concentrations of **1a** and **1a**-2'-d_1 were determined from total conversion, obtained by integration of the peaks in the LC spectrum corresponding to **1a** + **1a**-2'-d_1 and **2a** + **2a**-7a-d_1 and from the isotopic ratios **1a:1a**-2'-d_1 and **2a:2a**-7a-d_1 determined from MS analysis of the corresponding LC peaks. Plots of ln[**1a**] and ln[**1a**-2'-d_1] versus time were linear to ~3 half lives with observed rate constants of $k_{obs} = 2.19 \pm 0.03 \times 10^{-3}$ s^{-1} and $k_{obs} = 2.51 \pm 0.05 \times 10^{-3}$ s^{-1}, respectively (Figure 6), which correspond to an inverse KIE of $k_D/k_H = 1.15 \pm 0.03$.

Supplementary Material

Refer to Web version on PubMed Central for supplementary material.

Acknowledgments

Acknowledgment is made to the NIH (GM-080422) for support of this research and to the NCBC (2008-IDG-1010) for support of the Duke University NMR facility. We thank Dr. Marina G. Dickens for obtaining the X-ray crystal structure of **2a**. REMB thanks Duke University of a Burroughs Wellcome fellowship.

References

1. (a) Müller TE, Hultzsch KC, Yus M, Foubelo F, Tada M. Chem. Rev. 2008; 108:3795–3892. [PubMed: 18729420] (b) Widenhoefer RA, Han X. Eur. J. Org. Chem. 2006:4555–4563.(c) Pohlki F, Doye S. Chem. Soc. Rev. 2003; 32:104–114. [PubMed: 12683107] (d) Hong S, Marks TJ. Acc. Chem. Res. 2004; 37:673–686. [PubMed: 15379583]
2. (a) Marcsekova K, Doye S. Synthesis. 2007:145–154.(b) Anderson LL, Arnold J, Bergman RG. J. Am. Chem. Soc. 2005; 127:14542–14543. [PubMed: 16231885] (c) Beller M, Thiel OL, Trauthwein H. Synlett. 1999:243–245.(d) Yin Y, Zhao G. J. Fluorine Chem. 2007; 128:40–45.(e) Haskins CM, Knight DW. Chem. Commun. 2002:2724–2725.(f) Yin Y, Zhao GG. Heterocycles. 2006; 68:23–31.(g) Motokura K, Nakagiri N, Mori K, Mizugaki T, Ebitani K, Jitsukawa K, Kaneda K. Org. Lett. 2006; 8:4617–4620. [PubMed: 16986964] (h) Yang L, Xu LW, Xia CG. Tetrahedron Lett. 2008; 49:2882–2885.(i) Jimenez O, Muller TE, Schwieger W, Lercher JA. J. Catal. 2006; 239:42–50.(j) Ackermann L, Kaspar LT, Althammer A. Org. Biomol. Chem. 2007; 5:1975–1978. [PubMed: 17551648] (k) Jazzar R, Dewhurst RD, Bourg JB, Donnadieu B, Canac Y, Bertrand G. Angew. Chem. Int. Ed. 2007; 46:2899–2902.(l) Lapis AAM, DaSilveira Neto BA, Scholten JD, Nachtigall FA, Eberlin MN, Dupont J. Tetrahedron Lett. 2006; 47:6775–6779.(m) Yadav JS, Reddy BVS, Raju A, Ravindar K, Narender R. Lett. Org. Chem. 2008; 5:651–654.(n) Yang L, Xu LW, Xia CG. Synthesis. 2009:1969–1974.(o) Griffiths-Jones CM, Knight DW. Tetrahedron. 2010; 66:4150–4166.(p) Ackermann L, Althammer A. Synlett. 2008:995–998.
3. (a) Lemechko P, Grau F, Antoniotti S, Duñach E. Tetrahedron Lett. 2007; 48:5731–5734.(b) Coulombela L, Duñach E. Green Chem. 2004; 6:499–501.(c) Franck X, Figadere B, Cavé A. Tetrahedron Lett. 1997; 38:1413–1414.(d) Miura K, Hondo T, Takahashi T, Hosomi A. Tetrahedron Lett. 2000; 41:2129–2132.(e) Wang B, Gu Y, Yang L, Suo J, Kenichi O. Catal. Lett. 2004; 96:71–74.(f) Linares-Palomino PJ, Salido S, Altarejos J, Sanchez A. Tetrahedron Lett. 2003; 44:6651–6655.(g) Coulombel L, Duñach E. Synth. Commun. 2005; 35:153–160.(h) Zhou Y, Woo LK, Angelici RJ. Appl. Catal., A. 2007; 333:238–241.
4. Schlummer B, Hartwig JF. Org. Lett. 2002; 4:1471–1474. [PubMed: 11975606]
5. (a) Rosenfeld DC, Shekhar S, Takemiya A, Utsunomiya M, Hartwig JF. Org. Lett. 2006; 8:4179–4182. [PubMed: 16956181] (b) Li Z, Zhang J, Brouwer C, Yang CG, Reich NW, He C. Org. Lett. 2006; 8:4175–4178. [PubMed: 16956180]
6. (a) Taylor JG, Adrio LA, Hii KK. Dalton Trans. 2010; 39:1171–1175. [PubMed: 20104336] (b) Adrio LA, Quek LS, Taylor JG, Hii KK. Tetrahedron. 2009; 65:10334–10338.(c) McBee JL, Bell AT, Tilley TD. J. Am. Chem. Soc. 2008; 130:16562–16571. [PubMed: 19554728] (d) Cheng X, Xia Y, Wei H, Xu B, Zhang C, Li Y, Qian G, Zhang X, Li K, Li W. Eur. J. Org. Chem. 2008:1929–1936.(e) Taylor JG, Whittall N, Hii KK. Org. Lett. 2006; 8:3561–3564. [PubMed: 16869660] (f) Wei H, Qian G, Xia Y, Li K, Li Y, Li W. Eur. J. Org. Chem. 2007:4471–4474.(g) Wabnitz TC, Yu J-Q, Spencer JB. Chem. – Eur. J. 2004; 10:484–493.

7. (a) Chwang WK, Nowlan VJ, Tidwell TT. J. Am. Chem. Soc. 1977; 99:7233–7238.(b) Nowlan VJ, Tidwell TT. Acc. Chem. Res. 1977; 10:252–258.(c) Kresge AJ, Chiang Y, Fitzgerald PH, McDonald RS, Schmid GH. J. Am. Chem. Soc. 1971; 93:4907–4908.(d) Koshy KM, Roy D, Tidwell TT. J. Am. Chem. Soc. 1979; 101:357–363.(e) Csizmadia VM, Koshy KM, Lau KCM, McClelland RA, Nowlan VJ, Tidwell TT. J. Am. Chem. Soc. 1979; 101:974–979.(f) Chwang WK, Knittel P, Koshy KM, Tidwell TT. J. Am. Chem. Soc. 1977; 99:3395–3401.
8. (a) Taft RW. J. Am. Chem. Soc. 1952; 74:5372–5376.(b) Taft RW, Purlee EL, Riesz P, DeFazio CA. J. Am. Chem. Soc. 1955; 77:1584–1587.(c) Boyd RH, Taft RW, Wolfe AP, Christman DR. J. Am. Chem. Soc. 1960; 82:4729–4736.
9. (a) Freeman F. Chem. Rev. 1975; 75:439–490.(b) Banthorpe DV. Chem. Rev. 1970; 70:295–322.
10. (a) Cooper JD, Vitullo VP, Whalen DL. J. Am. Chem. Soc. 1971; 93:6294–6296.(b) Hevesi L, Piquard J-L, Wautier H. J. Am. Chem. Soc. 1981; 103:870–875.(c) Okuyama T, Fueno T. J. Am. Chem. Soc. 1980; 102:6590–6591.(d) Wautier H, Desauvage S, Hevesi L. J. Chem. Soc., Chem. Commun. 1981:738–739.
11. (a) Jencks WP. Chem. Rev. 1972; 72:705–718.(b) Jencks WP. Acc. Chem. Res. 1980; 13:161–169. (c) Jencks WP. Chem. Soc. Rev. 1981; 10:345–375.
12. Chiang Y, Kresge AJ. J. Am. Chem. Soc. 1985; 107:6363–6367.
13. Dietze PE, Jencks WP. J. Am. Chem. Soc. 1987; 109:2057–2062.
14. Herlihy KR. Aust. J. Chem. 1989; 42:1345–1350.
15. Fahey, RC. Topics in Stereochemistry. Eliel, EL.; Allinger, NL., editors. Vol. vol. 3. New York: Wiley-Interscience; 1968. p. 237-342.
16. (a) Hammond GS, Nevitt TD. J. Am. Chem. Soc. 1954; 76:4121–4123.(b) Hammond GS, Collins CH. J. Am. Chem. Soc. 1960; 82:4323–4327.
17. (a) Pocker Y, Stevens KD. J. Am. Chem. Soc. 1969; 91:4205–4210.(b) Weiss HM, Touchette KM. J. Chem. Soc., Perkin Trans. 1998; 26:1517–1522.
18. Fahey RC, McPherson CA. J. Am. Chem. Soc. 1971; 93:2445–2453.
19. Pasto DJ, Meyer GR, Lepeska B. J. Am. Chem. Soc. 1974; 96:1858–1866.
20. Becker KB, Grob CA. Synthesis. 1973; 12:789–790.
21. Fahey RC, Smith RA. J. Am. Chem. Soc. 1964; 86:5035–5036.
22. Fahey RC, Monahan MW. J. Am. Chem. Soc. 1970; 92:2816–2820.
23. Pasto DJ, Gadberry JF. J. Am. Chem. Soc. 1978; 100:1469–1473.
24. Staab HA, Wittig CM, Naab P. Chem. Ber. 1978; 111:2965–2981.
25. Naab P, Staab HA. Chem. Ber. 1978; 111:2982–2996.
26. Pocker Y, Stevens KD, Champoux JJ. J. Am. Chem. Soc. 1969; 91:4199–4205.
27. Fahey RC, McPherson CA, Smith RA. J. Am. Chem. Soc. 1974; 96:4534–4542.
28. Fahey RC, Monahan MW, McPherson CA. J. Am. Chem. Soc. 1970; 92:2810–2815.
29. (a) Corriu R, J Guenzet J. Tetrahedron. 1970; 26:671–684.(b) Fahey RC, McPherson CA. J. Am. Chem. Soc. 1969; 91:3865–3869.
30. Allen AD, Tidwell TT. J. Am. Chem. Soc. 1982; 104:3145–3149.
31. Roberts RMG. J. Chem. Soc., Perkin Trans. 1976; 2:1183–1190.
32. (a) Dewar JS, Fahey RC. Angew. Chem. Internat. Edit. 1964; 3:245–249.(b) Dewar JS, Fahey RC. J. Am. Chem. Soc. 1963; 85:3645–3648.(c) Abraham RJ, Monasterios JR. J. Chem. Soc., Perkin Trans. 1975; 2:574–578.(d) Berlin KD, Lyerla RO, Gibbs DE, Devlin JP. Chem. Comm. 1970:1246–1247.(e) Dewar JS, Fahey RC. J. Am. Chem. Soc. 1963; 85:2245–2248.(f) Dewar JS, Fahey RC. J. Am. Chem. Soc. 1963; 85:2248–2252.(g) Izawa K, Okuyama T, Fueno T. Bull. Chem. 1974; 47:1477–1479.
33. (a) Li X, Ye S, He C, Yu Z-X. Eur. J. Org. Chem. 2008:4296–4303.(b) Kovács G, Lledós A, Ujaque G. Organometallics. 2010; 29:5919–5926.
34. (a) Miura K, Hondo T, Nakagawa T, Takahashi T, Hosomi A. Org. Lett. 2000; 2:385–388. [PubMed: 10814329] (b) Miura K, Okajima S, Hondo T, Nakagawa T, Takahashi T, Hosomi A. J. Am. Chem. Soc. 2000; 122:11348–11357.
35. Zhang J, Yang C-G, He C. J. Am. Chem. Soc. 2006; 128:1798–1799. [PubMed: 16464072]

36. Subsequent experimentation revealed that triflic acid-catalyzed cyclization of substrates **1** occurs at lower temperature and with shorter reaction time (60 °C, 3 h) with the same stereochemical outcome.
37. X-ray data for **2a**: Monoclinic, P2(1)/c, T = 296 K, a = 8.8385(10) Å, **b** = 26.705(3) Å, c = 9.4913(11) Å, β = 94.690(8)°, V = 2232.8(5) Å^3, Z = 4, $R[F^2 > 2\sigma(F^2)]$ = 0.042, w$R(F^2)$ = 0.138. CCDC-798744 contains the supplementary crystallographic data for this paper. These data can be obtained free of charge from The Cambridge Crystallographic Data Centre via www.ccdc.cam.ac.uk/data_request/cif.
38. We were unable to assign the relative configuration of **2a**-3a,7$_{eq}$-d_2 from the H7a - H7$_{eq}$ and H7a - H7$_{ax}$ three-bond coupling constant as has been previously reported.[35] The equatorial conformation of the H7a proton leads to similar dihedral angles for H7a–C7a–C7–H7$_{eq}$ and H7a–C7a–C7–H7$_{ax}$. As a result, protons H7$_{eq}$ and H7$_{ax}$ display similar three-bond coupling constants to H7a of 4.8 Hz and 3.5 Hz, respectively, and both H7$_{eq}$ and H7$_{ax}$ display strong cross peaks to H7a in the ^{1}H-^{1}H NOESY spectrum. As such, the more reliable determinant to assign the H7$_{ax}$ and H7$_{eq}$ protons was the presence of a cross peak between H3 and H7$_{ax}$ and the absence of a cross peak between H3 and H7$_{eq}$ in the ^{1}H-^{1}H NOESY spectrum of **2a** (see Supporting Information).
39. The isotopomer **1a**-*N*-*d* was generated *in situ* by stirring a toluene solution of purified **1a** with D_2O at room temperature followed by removal of the toluene solution via syringe; attempted isolation or purification of **1a**-*N*-*d* led to significant loss of deuterium. The deuterium content of **1a**-*N*-*d* (~90% *d*) was determined by ^{1}H NMR integration. Owing to the nominal solubility of water in toluene (0.033%), this sample also contained 7.9 μmol (~16 mM) D_2O.
40. Howells RD, McCown JD. Chem. Rev. 1977; 77:69–92.
41. Laughlin RG. J. Am. Chem. Soc. 1967; 89:4268–4271.
42. Olavi P, Virtanen I, Maikkula M. Tetrahedron Lett. 1968; 9:4855–4858.
43. (a) Birchall T, Gillespie RJ. Can. J. Chem. 1963; 41:2642–2650.(b) Menger FM, Mandell L. J. Am. Chem. Soc. 1967; 89:4424–4426.
44. (a) Melander, L.; Saunders, WH, Jr. Reaction Rates of Isotopic Molecules. New York: Wiley; 1980. (b) Hengge, AC. Secondary Isotope Effects. In: Kohen, A.; Limbach, H., editors. Isotope Effects in Chemistry and Biology. Boca Raton: CRC; 2006. (c) Buncel, E.; Lee, CC., editors. Isotopes in Organic Chemistry, Vol. 7, Secondary and solvent isotope effects. Amsterdam: Elsevier; 1987. (d) Matsson O, Westaway KC. Adv. Phys. Org. Chem. 1998; 35:143–248.
45. Streitwieser A, Jagow RH, Fahey RC, Suzuki S. J. Am. Chem. Soc. 1958; 80:2326–2332.
46. For alternative explanations see: (a) Strauss OP, Safarik I, O'Callaghan WB, Gunning HE. J. Am. Chem. Soc. 1972; 94:1828–1834. (b) Safarik I, Strauss OP. J. Phys. Chem. 1978; 76:3613–3617. (c) Bender BS. J. Am. Chem. Soc. 1995; 117:11239–11246.
47. (a) Bigeleisen J. J. Chem. Phys. 1949; 17:675–678.(b) Bigeleisen J, Mayer MG. J. Chem. Phys. 1947; 15:261–267.(c) Bigeleisen J, Wolfsberg M. Adv. Chem. Phys. 1958; 1:15–76.
48. Values employed for *cis*-2-butene (cm^{-1}): 2980 (stretching), 1425 (in-plane bending), 852 (out-of-plane bending).[49] Values employed for secondary alcohol (cm^{-1}): 2900 (stretching), 1340 (in-plane binding), 1340 (out-of-plane bending).[49] See Supporting Information for additional details.
49. Roeges, NPG. A Guide to the Complete Interpretation of Infrared Spectra of Organic Structures. John Wiley & Sons; 1994.
50. (a) Hartshorn SR, Shiner VJ. J. Am. Chem. Soc. 1972; 94:9002–9012.(b) Gajewski JJ, Olson LP, Tupper KJ. J. Am. Chem. Soc. 1993; 115:4548–4553.(c) Okuyama T, Fueno T. J. Am. Chem. Soc. 1983; 105:4390–4395.
51. Hout RF, Levi BA, Hehre WJ. J. Comp. Chem. 1983; 4:499–505.
52. Seltzer S. J. Am. Chem. Soc. 1961; 83:1861–1865.
53. (a) Schubert WM, Lamm B, Keeffe JR. J. Am. Chem. Soc. 1964; 86:4727–4729.(b) Schubert WM, Lamm B. J. Am. Chem. Soc. 1966; 88:120–124.
54. Pocker Y, Hill MJ. J. Am. Chem. Soc. 1969; 91:7154–7158.
55. Kresge AJ, Weeks DP. J. Am. Chem. Soc. 1984; 106:7140–7143.
56. Collman, JP.; Hegedus, LS.; Norton, JR.; Finke, RG. Principles and Applications of Organotransition Metal Chemistry. Mill Valley, CA: University Science Books; 1987.

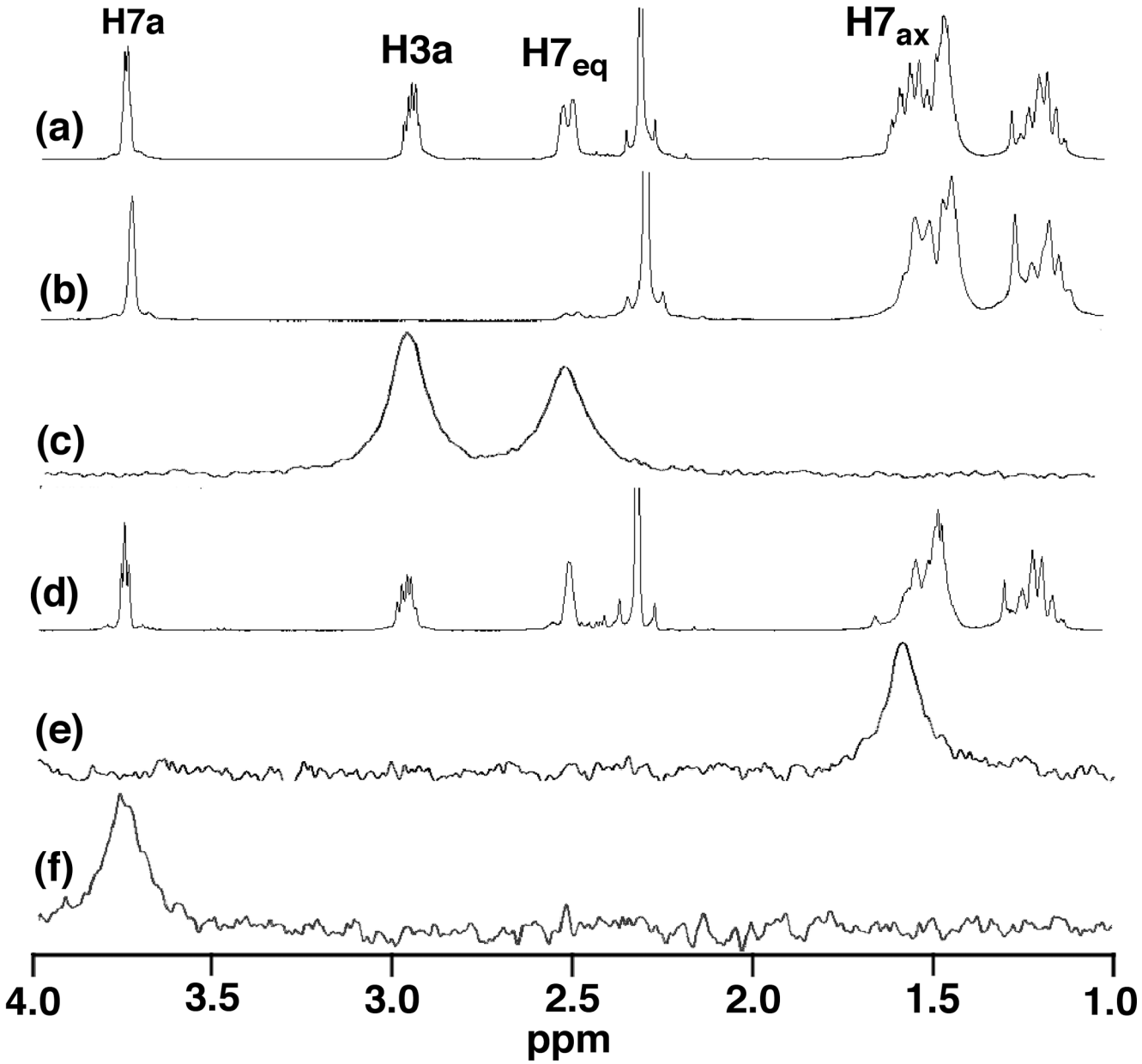

Figure 1.
Partial ^{1}H NMR Spectrum of 2a (a), Partial ^{1}H and ^{2}H NMR Spectra of 2a-3a,7$_{eq}$-d_2 (b and c), Partial ^{1}H and ^{2}H NMR Spectra of 2a-7$_{ax}$-d_1 (d and e), and Partial ^{2}H NMR Spectra of 2a-7a-d_1 (f)

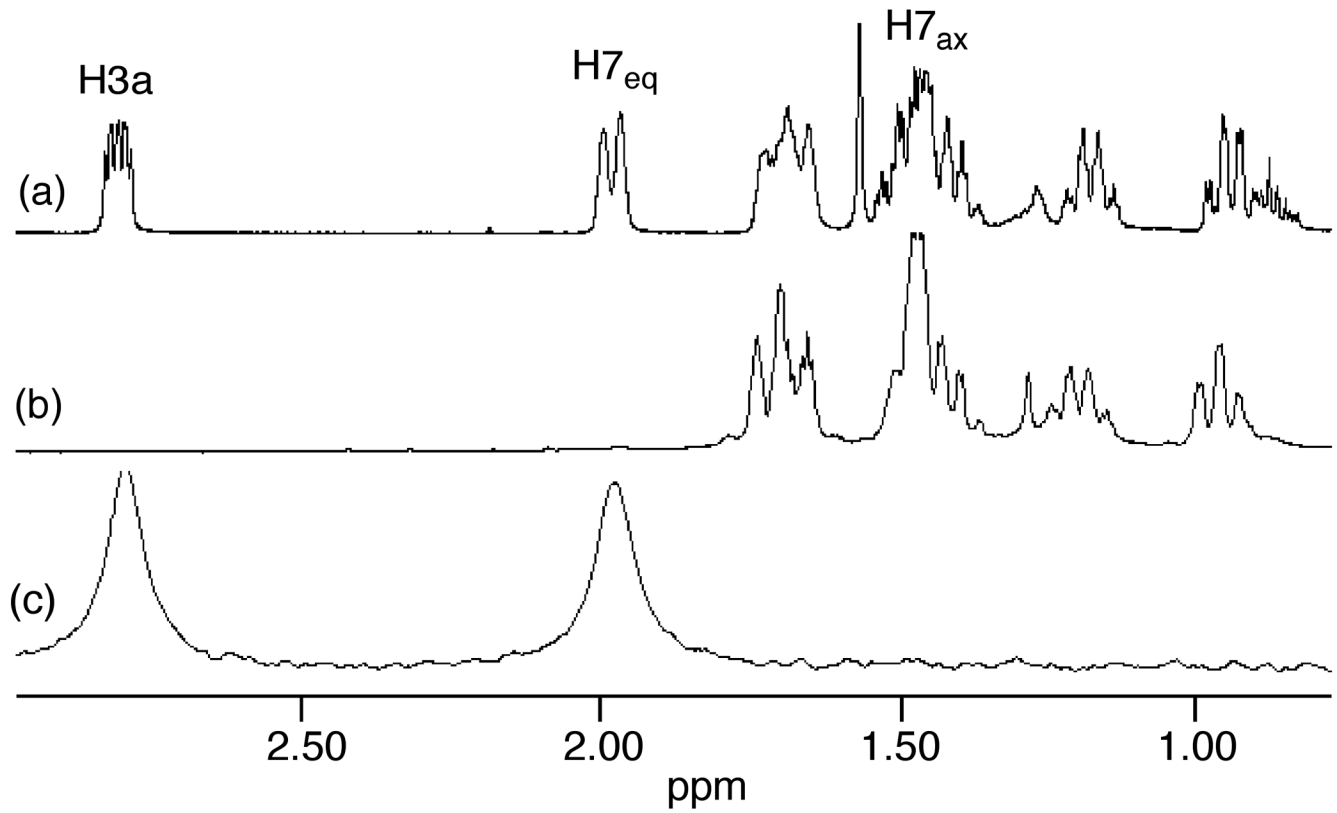

Figure 2.
Partial ^{1}H NMR Spectrum of **2b** (a) and Partial ^{1}H and ^{2}H NMR Spectra of **2b**-3a,7_{eq}-d_2 (b and c) and ^{2}H NMR Spectra of **2a**-7_{ax}-d_1 (d and e), and Partial ^{2}H NMR Spectra of $_{2a}$-7a-d_1 (f)

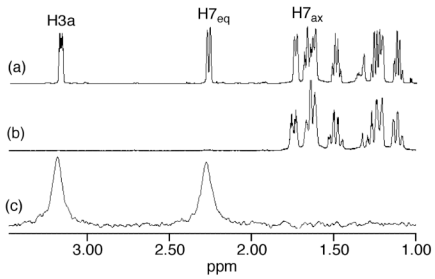

Figure 3.
Partial ^{1}H NMR Spectrum of **2c** (a) and Partial ^{1}H and ^{2}H NMR Spectra of **2c**-3a,7$_{eq}$-d_2 (b and c).

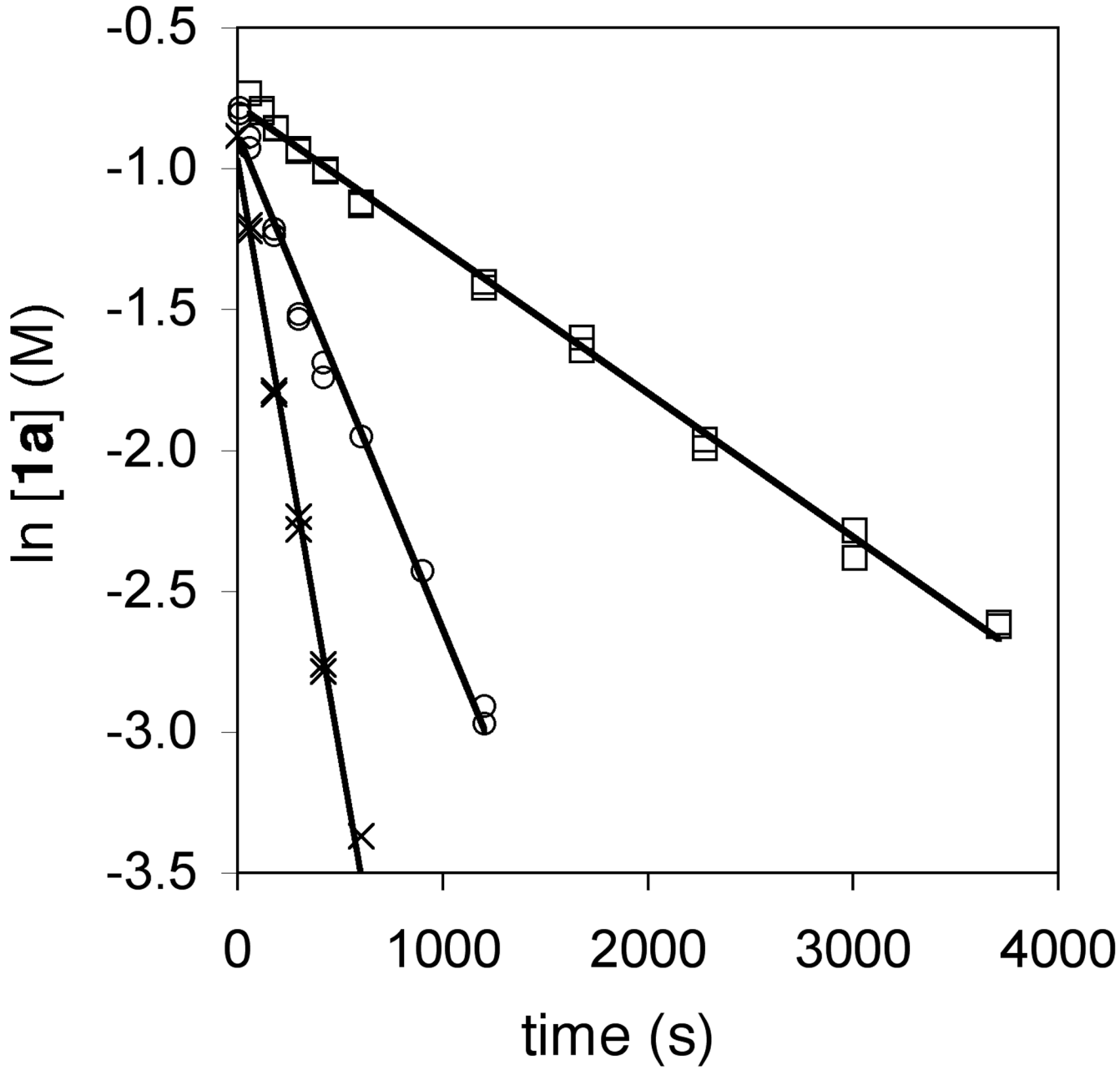

Figure 4.
First-Order Plots for the Conversion of **1a** ([**1a**]$_0$ = 0.50 M) to **2a** Catalyzed by Triflic Acid {[HOTf] = 5.0 (□), 12.6 (○), and 25.2 (×) mM} in Toluene at 62 °C

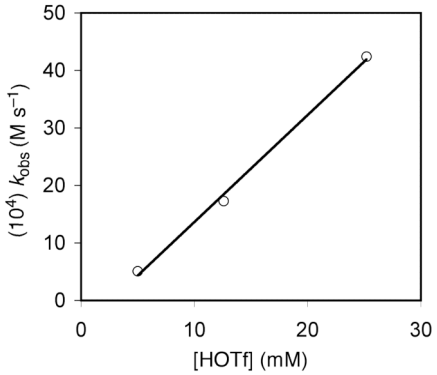

Figure 5.
Plot of k_{obs} Versus Triflic Acid Concentration for the Conversion of **1a** ($[\mathbf{1a}]_0$ = 0.5 M) to **2a** in Toluene at 62 °C

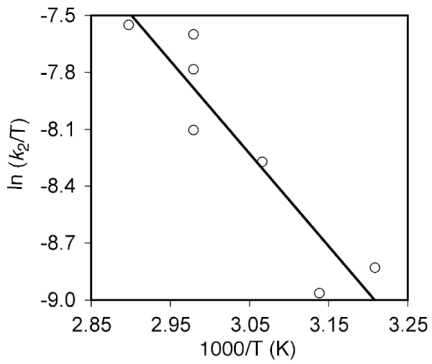

Figure 6.
Eyring Plot for the Conversion of **1a** ($[\mathbf{1a}]_0$ = 0.5 M) to **2a** Catalyzed by HOTf (25 mM) in Toluene over the Temperature Range 39–72 °C

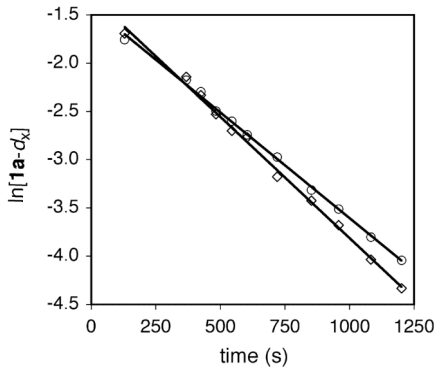

Figure 7.
First-Order Plots for the Conversion of **1a** to **2a** (○) and **1a**-2'-d_1 to **2a**-7a-d_1 (□), Catalyzed by Triflic Acid (5 mol %) in Toluene at 60 °C

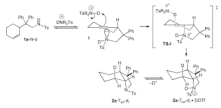

Scheme 1.
Proposed Mechanism of the DOTf-Catalyzed Cyclization of **1a**-*N*-*d*

Table 1

Brønsted Acid-Catalyzed Intramolecular Hydrofunctionalization of Substrates 1-d_2 at 85 °C for 48 h as a Function of Solvent and Acid (5 mol %).

entry	substrate	solvent	acid	product[a,b]	convn(%)[b]
1	1a-1’3’-d2	diglyme	HOTf	2a-3a,7eq-d2	≥95
2	1b-1’3’-d2	diglyme	HOTf	2b-3a,7eq-d2	≥95
3	1c-1’3’-d2	diglyme	HOTf	2c-3a,7eq-d2	≥95
4	1a-1’3’-d2	CH3CN	HOTf	2a-3a,7eq-d2	54
5	1b-1’3’-d2	CH3CN	HOTf	2b-3a,7eq-d2	36
6	1c-1’3’-d2	CH3CN	HOTf	2c-3a,7eq-d2	43
7	1a-1’3’-d2	toluene	HCl	2a-3a,7eq-d2	11
8	1b-1’3’-d2	toluene	HCl	2b-3a,7eq-d2	≤5
9	1c-1’3’-d2	toluene	HCl	2c-3a,7eq-d2	≤5
10	1a-1’3’-d2	toluene	TFA	2a-3a,7eq-d2	12
11	1b-1’3’-d2	toluene	TFA	2b-3a,7eq-d2	22
12	1c-1’3’-d2	toluene	TFA	2c-3a,7eq-d2	≤5

[a] Stereoselectivity was ≥90% in all cases.

[b] Conversion and stereoselectivity were determined by ^{1}H NMR of the purified reaction mixture.

Table 2

Observed Rate Constants for the Conversion of **1a** ($[\mathbf{1a}]_0$ = 0.5 M) to 2a Catalyzed by HOTf in Toluene as a Function of Temperature and [HOTf]

entry	[HOTf] (mM)	temp (°C)	(10^3) kobs (M^{s-1})
1	25	62.5	4.2 ± 0.1
2	12.6	62.5	1.54 ± 0.07
3	5.0	62.5	0.511 ± 0.007
4	25	38.5	1.15 ± 0.04
5	25	45.5	1.02 ± 0.03
6	25	53.0	2.10 ± 0.08
7	25	72.0	2.29 ± 0.07